Fussell, S. L., King, S. M., Royall, C. P., & Van Duijneveldt, J. S. (2022). Oxidative degradation of triblock-copolymer surfactant and its effects on self-assembly. *Journal of Colloid and Interface Science*, *606*, 953-960. https://doi.org/10.1016/j.jcis.2021.08.045

Journal of Colloid and Interface Science 606 (2022) 953–960

Contents lists available at ScienceDirect

Journal of Colloid and Interface Science

journal homepage: www.elsevier.com/locate/jcis

Oxidative degradation of triblock-copolymer surfactant and its effects on self-assembly

S.L. Fussell [a,c,d,*], S.M. King [b], C.P. Royall [a,c,d,e], J.S. van Duijneveldt [a]

[a] School of Chemistry, University of Bristol, Cantock's Close, Bristol BS8 1TS, UK
[b] ISIS Pulsed Neutron & Muon Source, STFC Rutherford Appleton Laboratory, Harwell Campus, Didcot, Oxon OX11 0QX, UK
[c] HH Wills Physics Laboratory, University of Bristol, Tyndall Avenue, Bristol BS8 1TL, UK
[d] Bristol Centre for Functional Nanomaterials, University of Bristol, Tyndall Avenue, Bristol BS8 1TL, UK
[e] Gulliver UMR CNRS 7083, ESPCI Paris, Université PSL, 75005 Paris, France

GRAPHICAL ABSTRACT

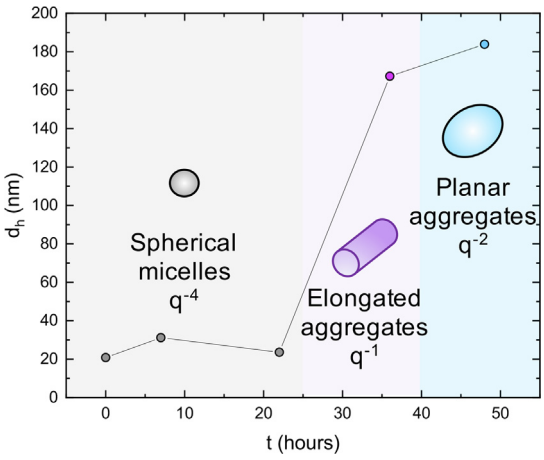

ARTICLE INFO

Article history:
Received 26 March 2021
Revised 4 August 2021
Accepted 7 August 2021
Available online 13 August 2021

Keywords:
Surfactant
Self-assembly
Gelation

ABSTRACT

We investigate the degradation behaviour of a triblock-copolymer surfactant made from polyethylene oxide (PEO) and polypropylene oxide (PPO) (PEO-PPO-PEO), highlighting how the aggregation behaviour of this polymer in water alters with ageing. Samples aged at room temperature were compared to samples degraded using accelerated ageing at elevated temperatures. We find that large mass losses occurred to the polymer surfactant which resulted in a change in the aggregation behaviour, with larger, rod-like or planar aggregates forming at longer degradation times. We look at how this change in aggregation behaviour changes the formulation stability of these polymers, specifically, the interaction of the polymer surfactant with poly(N-isopropylacrylamide) microgels. It is known that these species associate and form gels at elevated temperatures. This paper highlights how commonly used polymeric surfactants can degrade over time, resulting in dramatic changes to aggregation behaviour and therefore, formulation properties.

* Corresponding author at: School of Chemistry, University of Bristol, Cantock's Close, Bristol BS8 1TS, UK.
E-mail address: sian.fussell@bristol.ac.uk (S.L. Fussell).

https://doi.org/10.1016/j.jcis.2021.08.045
0021-9797/

1. Introduction

Poloxamer surfactants are a type of triblock-copolymer made from polyethylene oxide (PEO) and polypropylene oxide (PPO) (PEO-PPO-PEO), and are commonly found in many industrial products such as cosmetics, cleaning products and lubricants. They have several trade names including Pluronic and Synperonic surfactant. Their broad application range is due to the ability to optimise the polymer properties by controlling the ratio of the PPO: PEO blocks and the molecular weight. It is known that polymers degrade over time, both by thermal and oxidative degradation [1,2]. This degradation normally results in the loss of molecular weight from the polymer, either due to monomer units breaking off the end of the chain or chain scission [3]. Any changes to the molecular weight or ratio of PPO: PEO in these polymer systems is likely to influence the behaviour of these polymers. In this work, we investigate the thermal and room temperature degradation of a polymeric surfactant.

Formulation stability is of great importance in industrial chemistry, in sectors such as pharmaceuticals [4], agriculture [5] and applications such as engine oil additives [6]. Chemical formulations are often complex mixtures containing a wide variety of components. Any small changes to the chemical nature or composition of the formulation can alter the phase behaviour of the overall mixture, leading to instability. Colloidal flocculation is often a concern in formulations [7], as colloids are relatively large particles in the formulation that are prone to sediment or to form a gel under certain conditions [8]. If this happens post processing, it can significantly limit the shelf life of products. In solution, changes to the structure of polymers such as the molecular weight leads to changes in viscosity, solubility and the self assembly properties. In order to ensure product quality over the desired shelf life the degradation and resultant phase behaviour of these formulations needs to be understood.

The degradation of both PEO and PPO has been investigated in the literature [9–12]. These studies have identified the mechanism for oxidative thermal degradation in these polymers, where chain scission is the dominant degradation mechanism [13]. Both the products lost during the degradation process and the structure of the residual chain, have been investigated [14]. For high temperature degradation of PEO, the main products observed are formaldehyde and ethanol. However, differences are observed between the degradation of PEO and PPO, where the main degradation products of PPO through pyrolysis are acetaldehyde and acetone [14].

Here, we investigate how the properties of a poloxamer (PEO-PPO-PEO) change, through both room temperature and elevated temperature degradation. We show how degradation alters the molecular weight and therefore the aggregation behaviour of these aged polymers. We also highlight how the degradation of a triblock-copolymer surfactant can drastically alter the properties of formulations, due to the changes in aggregation behaviour and oxidation of the polymer chain. We use a formulation with a known phase behaviour to test this, by mixing the triblock-copolymer surfactant with poly(N-isopropylacrylamide) (pNIPAM) microgels. This formulation is known to form temperature responsive gels [15], however in the presence of degradation products, these gels form at considerably lower concentrations. This is important because pNIPAM microgels have become increasingly popular in polymeric applications, where undesired gelation could have a drastic impact on the processing and the application of these samples. Such gelation is particularly important for biomedical applications, where both of these species are extensively used [16,17].

Throughout this manuscript, the older polymer sample (10 years) will be referred to as the *aged polymer*, and the artificially aged polymer, degraded with temperature will be referred to as the *degraded polymer*.

This paper is organised as follows: we highlight the change in aggregation behaviour as a function of degradation using both imaging and scattering techniques in Section 3.1. This is followed by chemical analysis of the degraded polymer, including mass spectrometry and NMR in Sections 3.2 and 3.3 respectively. In 3.4 we compare the properties of the degraded and aged polymer. Finally we look at the change in phase behaviour of the aged polymer in the presence of pNIPAM microgels in Section 3.5.

2. Methods

2.1. Materials

N,N'-Methylenebis(acrylamide) (99% Sigma Aldrich), N-isopropylacrylamide (99% Acros Organics), potassium persulfate (>99% Sigma Aldrich), and sodium dodecylbenzenesulfonate (technical grade Sigma Aldrich) were used for the microgel synthesis. All chemicals were used as received without further purification.

The triblock-copolymer used for the artificial ageing studies was Synperonic PE/105 (PEO_{37}-PPO_{56}-PEO_{37}), supplied by Croda. The nominal molecular weight is 6500 g/mol. The polymer is 50 wt% PEO and 50 wt% PPO. To artificially degrade the triblock-copolymer surfactant, samples were weighed into an aluminium pan then placed in an oven, at either 75 °C or 80 °C At this temperature the polymer is a melt, the pour point is 35 °C.[18] Each sample was left at this temperature for a specific amount of time and the difference in mass of the triblock-copolymer was recorded. The samples were then decanted into sealed vials and stored at room temperature for further analysis.

The naturally aged polymer had been left in a container, opened a decade ago and stored at room temperature. The sample had been opened and resealed multiple times over the course of its lifetime. Both the aged and degraded polymer had a similar consistency, a soft deformable wax rather than the hard solid phase observed for the unaged polymer batch. The aged Synperonic PE/P105 was supplied by ICI surfactants.

2.2. Microgel synthesis

The pNIPAM microgels were synthesised using precipitation polymerisation, adapted from the methods reported by McPhee et al. 12.5 g of N-isopropylacrylamide, 1.0 g of N,N'-methylenebis (acrylamide) and 0.5 g of sodium dodecyl benzenesulfonate were added to a 1 L round bottom flask along with 475 mL of deionised water, fitted with an overhead stirrer and under an argon atmosphere. The solution was then heated to 70 °C. 0.5 g of potassium persulfate was added to the mixture as a 2 wt% solution. The microgels were then dialysed against deionised water for two weeks with daily water changes.

2.3. Scattering techniques

All dynamic light scattering (DLS) and static light scattering (SLS) data for the triblock-copolymer surfactant samples were characterised using a Malvern Autosizer 4800, with a 532 nm laser. For DLS, the samples were all run at multiple scattering angles, ranging from 30 to 130° in 10° intervals. For SLS, the intensity was measured at angles varying from 30 to 140° and 40 measurements were taken between each of these angles. Samples were diluted to 2.5 wt% using deionised water and the scattering recorded to see whether there was evidence of micelles present

in the samples. The critical micelle concentration (CMC) of Synperonic PE/105 is 0.3 wt% at 25 °C [15].

The larger triblock-copolymer surfactant aggregates took a long time to equilibrate, therefore the samples were prepared six days prior to analysis using DLS, where the size appeared to no longer alter with time.

The small angle neutron scattering (SANS) data was collected using the ZOOM beam line at the ISIS pulsed neutron source. The samples were run at one contrast, a 80:20 D_2O:H_2O mixture by mass and in 2 mm quartz cuvettes (Hell-ma, UK). Samples were prepared using H-Synperonic PE/P 105, one freshly opened and one that has been ageing for approximately a decade. The concentration of the samples was 0.75 wt%. Samples were run at 25 °C. The scattering data was collected for 20–40 μamp-hours (30–60 min). Separate transmission measurements were run for 6 μ-amp-hours (9 min). The wavelength range used was 1.75–15 Å with a sample-detector distance of 8 m. The SANS data were processed using the Mantid framework (version 5.0.1, https://www.matidproject.org) and then fit to several particle shape models including a homogeneous sphere model, available through SasView 5.0.3 (https://www.sasview.org). q is the scattering vector ($q = (4\pi\eta/\lambda)sin\theta$), the neutron refractive index (η) of these samples is approximated to be 1.

2.4. Microscopy

For confocal microscopy, all images were taken using a Leica (SP-5) confocal microscope. All samples were labelled with a Nile red dye, and a 543 nm HeNe laser was used to excite the dye. A 1 M Nile red solution was prepared in methanol, 10 μL of this was then added to a 2 mL, 2.5 wt% polymer solution dissolved in water. These samples were left stirring overnight to ensure equilibration. The microscopy samples were all prepared by adding a drop of sample to the centre of a doughnut shaped sticker attached to a microscope slide, with a cover slip over the sample.

2.5. Chemical characterisation

MALDI mass spectrometry was conducted using a UltrafleXtreme ABI4700 (Bruker). The samples were dissolved in chloroform at a concentration of 1 mg/mL prior to injection. All NMR spectra were recorded with a 400 MHz Jeol ECS400. Each sample was dissolved in D_2O and then ^1H and ^{13}C spectra were collected. The concentration of each sample run was 100 mg/mL. Each spectrum was analysed using MNova (Mestrelab Research) software (v 1.0).

2.6. Phase behaviour

The phase behaviour of each sample was determined by weighing 0.5 g of each sample concentration measured into 1.75 mL sealed vials. The samples were then placed into a heated water bath at approximately 70 °C, left at this temperature for approximately 10 min, then the phase behaviour was visually determined and recorded.

3. Results and discussion

The mass loss over time during degradation is plotted in Fig. 1 along with the corresponding phase of the sample after cooling. During the first 48 h of degradation, minimal mass loss was observed (<2%). In the subsequent 90 h, there is a significant increase in mass loss of up to 90%.

As degradation times increase the phase/state of the copolymer progressively changes from a hard 'solid' to a more a deformable wax (up to 48 h, purple) and then at the longest times becomes a liquid (longer than 48 h, pink), evidence that the molecular weight is decreasing with increased heating times [19]. This is common for heated polymers, where at elevated temperatures polymers undergo random chain scission [20].

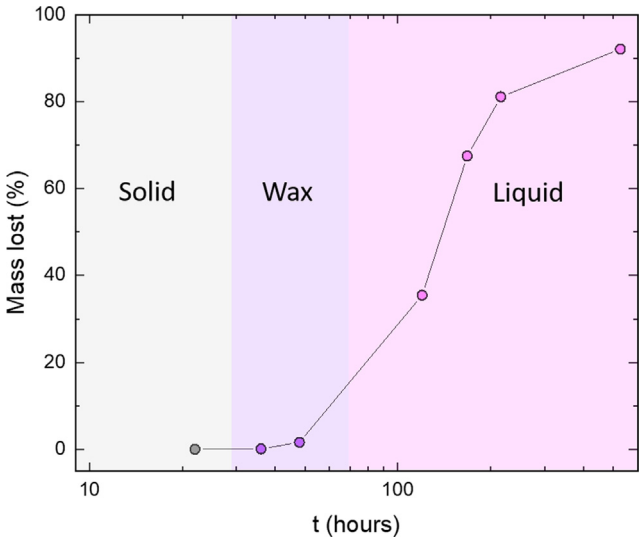

Fig. 1. Figure showing the mass lost from the triblock-copolymer undergoing degradation (Synperonic PE/P105) at 80 °C, as a function of time kept at temperature. The mass loss is reported as a percentage of the original mass of the sample. The pink and purple data points indicate samples that at room temperature, are a liquid and wax respectively, and the grey data points represent samples that remain a hard solid.

3.1. Aggregation behaviour

We investigated the aggregation behaviour of the degraded polymers using light scattering techniques (Fig. 2). An interesting observation was that the aggregation behaviour of the triblock-copolymers appeared to change with degradation time. The angular dependence of the scattering from objects gives an indication of

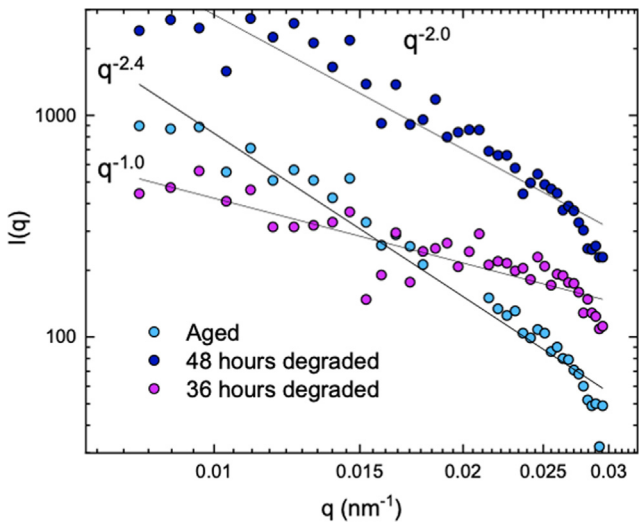

Fig. 2. Figure showing SLS data for both the artificially degraded and aged triblock-copolymer samples. The degraded samples were artificially degraded at 80 °C. The scattering data was collected at 25 °C. The lines are the power law fits to the SLS data. The q dependence calculated from the gradient is included next to each fit. The figure shows triblock-copolymer degraded for 36 h (purple) and for 48 h (navy), both at 80 °C. The light blue data is the aged polymer. The concentration is 2.5 wt% triblock-copolymer for all samples.

the structure. This dependence varies with q^{-d}, where d is related to the fractal dimension of the scattering object. For the sample that has been aged for 36 h, the SLS intensity varies with a q^{-1} dependence, which is consistent with the presence of elongated objects such as cylindrical micelles. For samples that have been aged for 48 h, the q dependence observed was q^{-2}, which suggests that planar (2D) aggregates are present in solution. This could reflect aggregated cylindrical micelles, more ellipsoidal micelles or planar objects such as rafts or sheets. Poorly-solvated polymer chains can also present a q^{-2} dependence, but the presence of these is incompatible with the DLS and SANS data which points to some degree of self-assembly.

The DLS diameter of the triblock-copolymer micelles was found to increase with increasing degradation time, to sizes much larger than is typical of spherical triblock-copolymer micelles (c.a. 20 nm [15]). The diameter increased to 180 nm, for samples that had been left at 80 °C for 48 h. Samples that had been left for longer degradation times (>120 h) gave an unclear DLS reading, but the correlation function indicated that the objects were less ordered and polydisperse.

DLS is routinely used to study spherical particles, where there is only one contribution to the translational diffusion coefficient, therefore the diffusion coefficient directly gives the hydrodynamic radius of the particle [21]. The SLS indicated that the objects were non-spherical and as a result, interpretation of the DLS data is less straightforward. DLS gave an angle dependent hydrodynamic diameter for the micelles, which also suggests the objects are no longer spherical, but instead have multiple contributions to the diffusion coefficient [22]. This angular dependence was only observed when an increase in the hydrodynamic radius was also observed at 90°. The results are summarised in the ESI (Fig. S3. ESI). Visual observations of macroscopic samples were consistent with the light scattering data. The unaged samples were clear; DLS and SLS indicated that spherical micelles were present. For the samples aged longer than 36 h, there was an indication of larger scattering objects as the opacity of the sample increased. For the longest aged samples (>120 h), where DLS indicated that no scattering objects were present, these samples again became clear.

We imaged the degraded triblock-copolymer samples using confocal microscopy to see if we could obtain further information about the size and shape of the aggregates formed. The results complemented the DLS data (Fig. S10 ESI). When the unaged sample was imaged, there was no obvious sign of aggregates, due to the small size of the spherical triblock-copolymer micelles. A similar micrograph was obtained for the sample that has been aged for 36 h. This is as expected as the light scattering data indicates the aggregates are 1D objects of order 200 nm, which again would not be resolvable on a standard confocal microscope. For the sample that was aged for 48 h, there was evidence of larger aggregates, where the average size was 600 nm in diameter. The size of the aggregates at 36 and 48 h were similar in diameter when measured on the DLS, this indicates that the difference in shape is likely to be the cause of whether the samples can be resolved using confocal microscopy, as 1D objects will be less resolvable than 2D objects using confocal microscopy. This supports the hypothesis that the shape of the aggregates obtained changes with degradation time. Samples degraded for 120 h did not show evidence of aggregates using confocal microscopy, consistent with the DLS data. This is likely due to these polymers being heavily degraded and therefore are no longer acting as surfactants.

A scheme summarising this change in aggregation with increased degradation along with the DLS data carried out at 90° has been included in Fig. 3, to highlight how the increase in size correlates to the shape of the object identified from SLS.

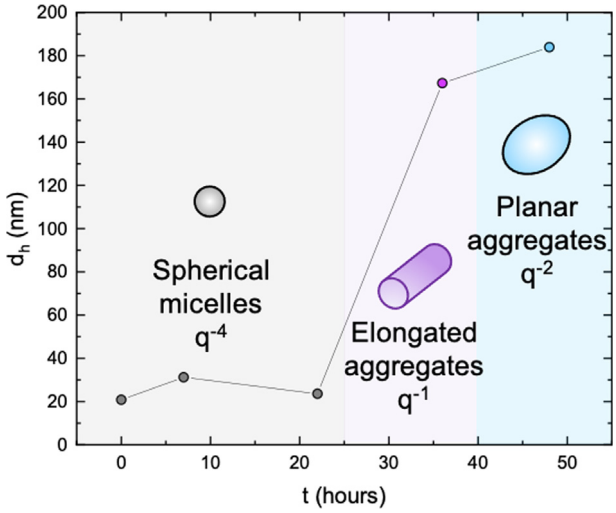

Fig. 3. Apparent size dependence of the triblock-copolymer micelles as a function of the artificial ageing time when degraded at 80 °C. The predicted shape of the aggregates deduced from SLS has been included to highlight how the aggregation behaviour changes with ageing. All the DLS data were taken at 25 °C and at 90° detector angle. The grey data represents spherical or ellipsoidal micelles, the purple data elongated objects (1D) and the blue data planar objects (2D).

3.2. Mass spectrometry

In order to understand the chemistry underlying this change in aggregation behaviour, samples of the degraded polymer were characterised using MALDI mass spectrometry. The full MALDI mass spectra are included in the ESI, including zoomed in regions to highlight the peak spacing (Fig. S15-21). Mass spectrometry indicated the molecular weight distribution in the polymer samples shifted to considerably lower masses with increased ageing, even when there was minimal mass loss observed in the macroscopic sample (less than 48 h Fig. 1). The range of masses observed are summarised in Fig. 4. For all samples, the mass spectra indi-

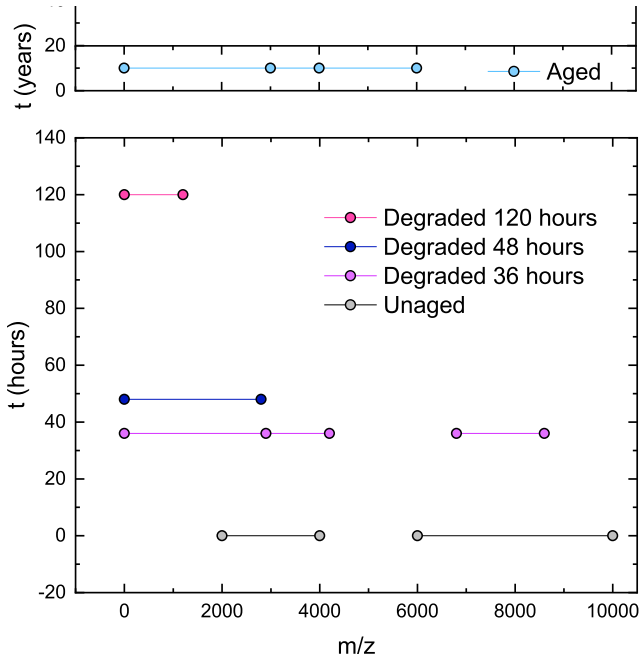

Fig. 4. Figure showing the mass ranges of the triblock-copolymer polymer obtained at different degradation times using MALDI mass spectrometry. All samples were degraded at 80 °C. The top panel (light blue) shows the mass ranges observed for the aged sample.

cated that a block-copolymer was still present in the sample. In the unaged polymer sample, the spacing was 14 mass units, consistent with the difference in mass between a PPO and a PEO segment. No other peak spacing was resolved in this spectra, likely due to the high molecular weight of the polymer and the roughly equal mass ratio of the two polymer blocks.

For samples aged for longer than 36 h, there was evidence of a 44 spacing, which is consistent with the PEO group, and a 58 spacing, consistent with the PPO group along with 44 spacing. The peaks with 44 spacing are at a higher intensity and the mass of these polymer peaks indicated that the polymer was very close to pure PEO. In the lower intensity peaks there is evidence of 58 spacing, consistent with PPO and 44 spacing. This could indicate that there are a mixture of polymeric species in solution, one that is nearly pure PEO and one/two that are a block-copolymer containing both PEO and PPO, with a higher ratio of PPO. This would result from the chain scission occurring primarily in the PEO region of the polymer, leaving a PEO chain and a PPO block-copolymer with a higher proportion of PPO than PEO.

3.3. Chemical analysis

The thermally degraded samples were also studied using NMR spectroscopy, to identify the composition of the samples remaining after degradation and further understand the changes to the aggregation behaviour. Samples were studied using ^{13}C and ^{1}H NMR. In the ^{13}C spectra of the unaged sample, the expected NMR peaks are present. There is a large peak at 69.7 ppm for the CH_2 carbons in the PEO chains, with further peaks at 75.3, 73.0, 17.32 ppm for the CH, CH_2 and CH_3 respectively for the PPO carbons. There is also a peak at 60.5 ppm which is likely the CH_2 in the end group next to the OH. This peak has a relatively small intensity, which is expected for polymeric species with a reasonably high molecular weight. The ^{13}C spectra for a unaged triblock-copolymer sample is included in Fig. 5 (blue).

The relative intensities of the end groups of the degraded polymers were quantified using ^{13}C NMR. All fractions are relative to the signal from the PEO CH_2 (69.7 ppm). It was observed that with increasing degradation time there is an increase in the number of end groups present, and there is an increase in the fraction of end groups relative to the polymer back bone carbons. This is highlighted in Fig. 5, where the end group peaks are labelled with an asterisk. All of the end groups appear to be the result of oxidative chain scission. This shows how the molecular weight of the polymer decreases with increasing degradation time, through random chain scission. For PEO, the main degradation products are hydroxy, methoxy and formate. For PPO acetate is also one of the main degradation products that is not seen for the degradation of PEO. The mechanism for oxidative chain scission is included in the ESI (Fig. S24 ESI). Like MALDI, all of the NMR spectra showed evidence that both PEO and PPO were present in the sample: the main chain peaks remained present in the spectra, and the fraction of each changed little (Fig. S25 ESI). These main chain peaks do broaden with increasing degradation.

The fraction of end groups increased with increasing degradation time. Some example end group fractions obtained for the different masses are included in Fig. 5. This includes the hydroxy end group -CH_2OH found for PEO degradation (60.5 ppm), the formate group that is found for both PEO and PPO degradation -COH (166.5 ppm), and the acetate or formate beta carbon associated with PPO degradation. We observed that there was a difference in the relative amounts of each end group, and this was attributed to the scission occurring preferentially in the PEO region of the polymer. The highest concentration end group appears to be the CH_2OH hydroxy group, which is present in the polymer before degradation and increases in concentration with continued degradation. This end group is found in the PEO segment of the polymer chain and is also formed from the oxidative degradation of PEO. The second highest concentration end group appears to be the formate group CHO, this group results from the oxidative degradation of both PPO and PEO. There is also evidence of end groups that are only associated with the degradation of PPO, which are acetate end groups, however these are present at much lower concentrations than the end groups associated with PEO. There is further evidence of the acetate peak forming in the ^{1}H NMR spectra of the degraded polymers, where a peak for acetate CH_3 hydrogens is present at

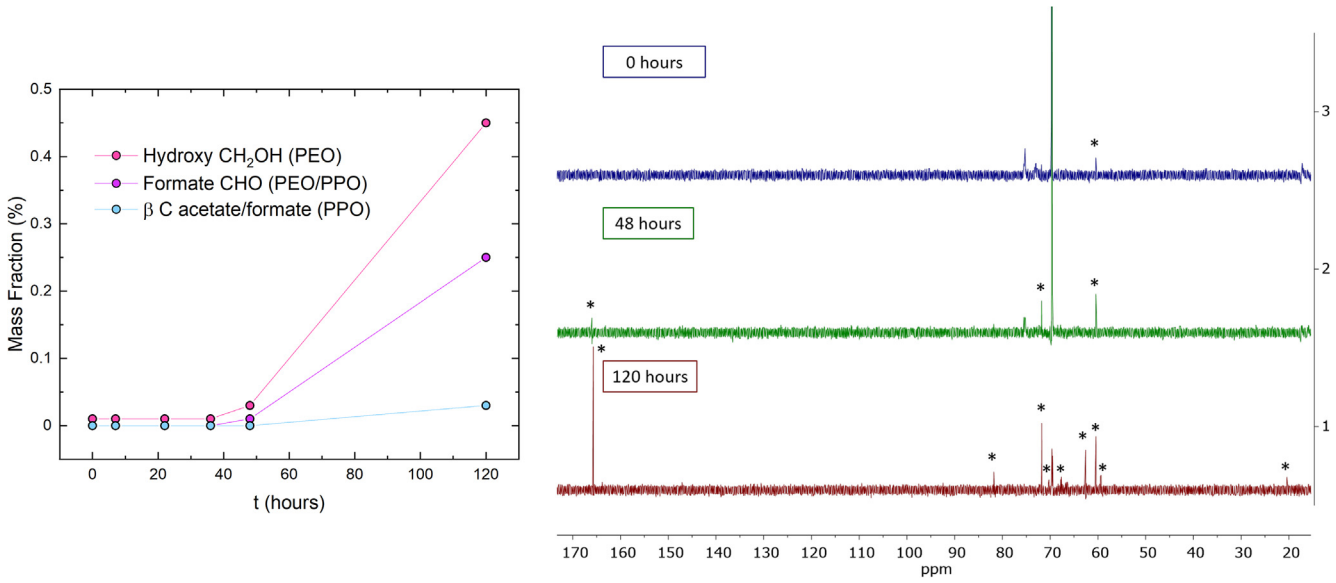

Fig. 5. (Right) figure showing the ^{13}C NMR spectra for the degraded triblock-copolymer surfactant at different degradation times. The samples have been aged in an oven at 80 °C in air. The blue spectra is of the unaged sample, the green spectra is of a sample aged for 48 h, and the red spectra is of a sample that has been aged for 120 h. The peaks with an asterisk above them are the end group peaks. (Left) figure showing the mass fraction of each end group identified in the triblock-copolymer as a function of degradation time. The blue curve is for the alcohol end group, at 60.43 ppm. The purple curve is for the formate end group, at 166.5 ppm, and the pink curve is for the methoxy end group, found at 71.8 ppm. Each fraction is compared to the PEO main chain CH_2 peak at 69.5 ppm.

approximately 2 ppm (ESI Fig. S30). From this data it was concluded that the scission preferentially occurs in the PEO segment of the polymer, but there is evidence of this scission occurring in both polymer regions.

The sample degraded for 120 h has the most extreme degradation when looking at the NMR spectra. This is highlighted in Fig. 5. There are multiple back bone peaks present and the fraction of end group carbons is comparable to the number of back bone carbons. It appears from the NMR that only low molecular weight polymers and oligomers remain after the longest degradation times. This is consistent with the DLS data obtained for this sample, where the scattering indicated that no aggregates were present.

3.3.1. Comparisons of chemical degradation to the changes in aggregation behaviour

The NMR data indicates that with increasing degradation time, there is an increase in the number of end groups, highlighting that the molecular weight of the polymer units is decreasing. As the triblock-copolymer is a surfactant, any alterations to the structure of the polymer is likely to alter the packing parameter of the surfactant [23]. If the polymer scission results in the loss of mass from the PEO region of the polymer, then this would result in the area of the head group decreasing with respect to the size of the surfactant tail. This would result in the packing parameter increasing, an effect known to promote the formation of cylindrical micelles. The decrease in the amount of PEO in the polymer will also promote the formation of larger aggregates, as the increasingly hydrophobic molecules will prefer to self-assemble into larger objects to protect the structures from the water solvent. If the polymer scission occurs in the PPO segment of the polymer, the result would be the length and volume of the tail increasing compared to the head group area, which leads to spherical micelles being the preferred aggregate. However, if this was the scission mechanism, this would likely result in low molecular weight PPO species being present in solution which can cause micelles to swell. It was shown that a spherical to worm-like to lamellar phase transition was induced in triblock-copolymer mixtures upon the addition of small water insoluble molecules, such as low molecular weight diols [24]. Therefore scission in both segments of the polymer will promote the formation of swollen micellar structures. NMR showed that the scission occurs mostly in the PEO segment and to a lesser extent in the PPO one. MALDI also indicated that there was a higher concentration of PEO present in these samples over the mass range studied. The self-assembly routes described in Section 3.1 are therefore supported by the chemical changes to the polymer identified in the mass spectrometry and NMR data.

The alteration in the packing of these polymers could result from the formation of mixed micelles as the various polymer chains aggregate, which also results in the swelling of surfactant systems. It has also been shown in the literature that the addition of non-ionic surfactants to triblock-copolymer samples can induce the formation of cylindrical micelles and vesicles [25].

The consequence of these ageing effects for formulation stability and product processing needs to be considered when estimating the shelf life of materials. It is known that the viscosity of a cylindrical micelle in solution is considerably higher than that of spherical micelles. This would result in the need to alter processing conditions to account for this. These triblock-copolymers are considered non-toxic and several are FDA approved. How the degradation of the triblock-copolymer affects their toxicology has been investigated [26], with the focus on the formation of degradation products causing an increased toxicity to cells. It is also known that the size and shape of nanoparticles also effects their toxicology and biodistribution [27], therefore the changes to aggregation could also have an effect on the toxicity of these polymeric species [28].

3.4. Comparison between aged and degraded polymer behaviour

As part of this investigation, aged copolymers were compared to thermally degraded copolymers. The aged samples showed similar behaviour to the samples that had been artificially degraded for 48 h. Again, the angle resolved DLS indicated that non-spherical objects were present in the aged samples, as the hydrodynamic diameter varied with the scattering angle. This was highlighted by the hydrodynamic diameter decreasing with increasing scattering angle. The change in diameter across the angles measured was, however, less than for the artificially degraded sample. This is likely due to the lower size polydispersity measured for the aged sample compared to the artificially degraded sample. When carrying out SLS on the aged sample, the q dependence indicated that 2D polymer aggregates were present in solution (q^{-2}, Fig. 2). This shows that similar alterations to the self-assembly behaviour can be observed for polymers that have been degraded by both ageing and thermal degradation. The aged sample was also imaged using confocal microscopy and this again indicated the presence of larger aggregates of approximately 700 nm in diameter (Fig. S10 ESI).

A SANS investigation comparing the aged and unaged polymer was conducted to obtain further detail about the structural changes that occur to the micelles with ageing. This is summarised in Fig. 6. It was observed that with aging the scattering curve shifts to smaller q values, indicating an increase in the size of the micelles, as was seen with DLS. At the same time the aged sample also indicated the presence of even larger objects, giving rise to a q^{-2} dependence, as was seen with SLS. The size and shape of the micelles were examined by model-fitting the SANS data. Fig. 6 shows the fits to a homogeneous sphere model, to allow comparison with the DLS results, and which returned diameters of 11 nm and 15 nm for the unaged and aged samples, respectively. It is not unusual that DLS dimensions are larger than SANS-derived dimensions simply because the former also include the solvent molecules that diffuse with the micelle, but the data from the unaged sample was clearly comparable nonetheless. For the aged sample as a result of the different wave vector ranges, SANS allows us to see both the micelle signal at high q and the scattering due to the larger aggregates at low q. The static light scattering signal is dominated by the latter.

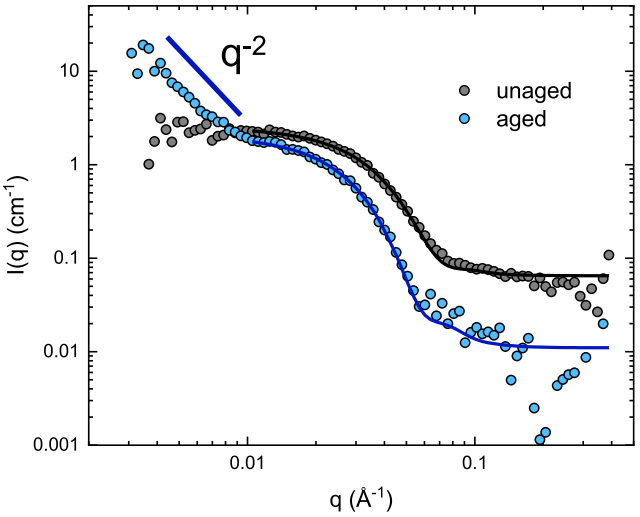

Fig. 6. SANS data obtained from aged and unaged triblock-copolymer. The solvent was 80% D_2O by mass, and 20% H_2O, the data was collected at 25 °C. The concentration of triblock-copolymer is 0.75 wt%. The fits were obtained using a homogeneous sphere model.

In the ESI alternative model fits to the SANS data, using models for a homogeneous ellipsoid and a core-shell ellipsoid, are shown. All three models fit the intermediate and high q SANS data very well, but it does seem that the ellipsoidal models are slightly better descriptions of the micelles than the spherical model, particularly in the case of the aged sample. Whilst the modest elongation ($\sim$ 2:1) suggested by the fitting is not, in itself, enough to explain the q^{-2} upturn in the low q scattering from the aged sample, it does hint at the possibility of a broader morphological transition leading to the presence of more planar structures or aggregates (e.g. oblate ellipsoids, lamellar rafts). But irrespective of the actual morphology, it is clear that the structure of the micelles alters significantly with aging.

Chemical analysis of the degradation that occurs in the aged polymer was also conducted. When looking at the MALDI mass spectra of the aged polymer there were similar differences in the molecular weight observed and peak spacing (Fig. S22-23 ESI). This indicates that the degradation process is very similar when comparing aged and thermally degraded samples. The NMR spectra obtained for the aged sample was again consistent with a sample degraded for approximately 36–48 h. The end groups are considerably more prominent than in the unaged triblock-copolymer sample. An NMR spectra comparing the unaged, thermally degraded and aged sample is included in the ESI (Fig. S31 ESI). There is evidence of scission occurring in both the PPO and PEO segment of the polymer, and again the scission appears to occur preferentially in the PEO region of the polymer. The fraction of end groups measured in the aged samples are included in the ESI (Fig. S25 ESI). From this it can be concluded that thermal degradation provides a suitable comparison to the ageing process of polymers, aged through oxidation degradation at room temperature, due to the comparable NMR and mass spectra obtained. This indicates, as with the artificially degraded polymer, that there is a large change in the polymer structure and molecular weight with ageing.

3.5. Formulation behaviour of degraded triblock-copolymer surfactant

In this work, we wanted to highlight the effects of polymer ageing on formulation properties. In order to achieve this we looked at the change in the interaction between the triblock-copolymer surfactant and pNIPAM microgels with degradation. In solution it is known that these polymers associate on heating, likely through hydrogen bonding [15]. This association results in the formation of space spanning gels that collapse over time, the result being a reversible temperature responsive gelation.

It was observed that with increased degradation time, the concentration at which the samples form temperature responsive gels decreases. This is summarised in Fig. S32 in the ESI. The association of the triblock-copolymer micelles and pNIPAM is thought to be due to hydrogen bonding between pNIPAM and the polymer surfactant. We have shown that with increasing degradation, the polymer becomes increasingly oxidised. This would also result in gelation occurring at lower concentrations, as the hydrogen bonding is enhanced between the two polymers. Another driver is likely to be the changes in the polymer composition, whereby the loss of PEO from the polymer leads to decreased solubility, resulting in the association of the polymers occurring more readily. The oxygenated polymer is also likely to have an associated charge, due to the formation of more acidic groups, which would result in the microgels becoming more prone to aggregation due to charge screening effects. The smaller molecules, due to the decrease in molecular weight will also more easily penetrate inside the microgel network. All of these could result in the gelation occurring at lower concentrations. When comparing the phase behaviour of the triblock-copolymer before and after ageing, the concentration where gels formed also lowered considerably, this is highlighted in Fig. S33 in the ESI.

Formulations containing both PEO and pNIPAM and poloxamer and pNIPAM are commonly found in the literature, where often the application is biomedical research [29,30]. This is due to the responsive nature of pNIPAM and the non toxic properties of poloxamer surfactants. The gelation that occurs in mixtures of these polymers could be desirable, for example for tissue engineering purposes [31]. However, especially for biomedical applications, the formation of solids could have detrimental results, for example for drug delivery vehicles [32]. The alterations in the concentration where gels are observed is an important characteristic to quantify when formulating these polymers and when considering these polymers for use in specific applications, especially where a long shelf life is required. This could have wider effects, where degradation could alter the behaviour of these polymers in a wide range of formulations. This could be through not only the altered flow properties, due to the changes in aggregation behaviour, but also the stability of formulations to sedimentation and gelation.

4. Conclusions

Our results have identified the degradation mechanism for a common poloxamer surfactant. It was known that molecules such as PEG and PPO undergo oxidative degradation [14]. Here however we have characterised both this chemical breakdown (using MS) and its impact on the self-assembly behaviour of a triblock-copolymer surfactant (using light and neutron scattering). The key observation was that with increased degradation time, the polymer molecular weight decreases, and elongated aggregates are observed. We related the structure of the self-assembled object observed to the individual degraded surfactant molecules. The self-assembly routes identified using scattering techniques are supported by the chemical changes to the polymer observed in the mass spectrometry and NMR data. This understanding of the degradation with both time and elevated temperature has important implications in a variety of applications, for formulation stability and, in particular, where biomedical application of the polymers are being investigated, as the toxicity of these polymer degradation products needs to be assessed.

CRediT authorship contribution statement

S.L. Fussell: Conceptualization, Methodology, Formal Analysis, Visualisation, Writing – original draft, Investigation, Writing – review & editing. **S.M. King** Resources, Date Curation, Formal Analysis, Writing – review & editing, Software. **C.P. Royall:** Supervision, Writing – review & editing. **J.S. van Duijneveldt:** Conceptualization, Supervision, Writing – review & editing.

Declaration of Competing Interest

The authors declare that they have no known competing financial interests or personal relationships that could have appeared to influence the work reported in this paper.

Acknowledgements

SF is funded by an EPSRC studentship (EP/L016648/1) provided by the Bristol Centre for Functional Nanomaterials. CPR acknowledges support from EPSRC grant (GR/M32320/01) and ERC consolidator grant NANOPRS 617266. We would like to thank the University of Bristol Mass spectroscopy facility for running the MALDI samples. We would also like to thank Craig Davies, Croda, for supplying the Synperonic PE/P105. We would like to thank

Jason Potticary for running the TGA analysis. The STFC is acknowledged for the provision of neutron beamtime at ISIS (Experiment number RB2010103; DOI: 10.5286/ISIS.E.RB2010103-1). This work benefited from the use of the SasView application, originally developed under NSF award DMR-0520547. SasView contains code developed with funding from the European Union's Horizon 2020 research and innovation program under the SINE2020 project, grant agreement No 654000.

Appendix A. Supplementary material

Supplementary data associated with this article can be found, in the online version, at https://doi.org/10.1016/j.jcis.2021.08.045.

References

[1] S.L. Madorsky, S. Straus, J. Res. Natl. Bureau Stand. Sect. Phys. Chem. 63A (1959) 261.
[2] J. Pospíšil, Z. Horák, Z. Kruliš, S. Nešpurek, S.I. Kuroda, Polym. Degrad. Stab. 65 (1999) 405–414.
[3] B.M. Fanconi, J. Appl. Phys. 54 (1983) 5577–5582.
[4] S. Bajaj, D. Singla, N. Sakhuja, J. Appl. Pharmaceut. Sci. 2 (2012) 129–138.
[5] S.T. Atwood, T.J. Sheets, T.B. Sutton, R.B. Leidy, J. Agric. Food. Chem. 35 (1987) 169–172.
[6] A.K. Tripathi, R. Vinu, Lubricants 3 (2015) 54–79.
[7] J. Matusiak, E. Grzdka, Annales Universitatis Mariae Curie-Sklodowska, sectio AA – Chemia 72 (2017) 33.
[8] N. Datta, H.C. Deeth, Food Bioprod. Process. Trans. Inst. Chem. Eng. Part C 79 (2001) 197–210.
[9] M. Duval, E. Gross, Macromolecules 46 (2013) 4972–4977.
[10] J.A. Giroto, A.C.S.C. Teixeira, C.A.O. Nascimento, R. Guardani, Ind. Eng. Chem. Res. 49 (2010) 3200–3206.
[11] S.P. Zustiak, J.B. Leach, Biomacromolecules 11 (2011) 1348–1357.
[12] L. Hill, E. Canning, S.A. Sell, S.P. Zustiak, J. Mater. Chem. B 5 (2017) 2679–2691.
[13] N. Grassie, G.A. Perdomo Mendoza, Polym. Degrad. Stab. 9 (1984) 155–165.
[14] T.G. Blease, R.I.G. Thompson, L.I. Yang, Eur. Polym. J. 32 (1996) 535–547.
[15] S.L. Fussell, K. Bayliss, C. Coops, L. Matthews, W. Li, W.H. Briscoe, M.A. Faers, C. P. Royall, J.S. van Duijneveldt, Soft Matter 15 (2019) 8578–8588.
[16] D.A. Links, Soft Matter 7 (2011) 6375–6384.
[17] S. Fusco, A. Borzacchiello, P.A. Netti, J. Bioactive Compatible Polym. 21 (2006) 149–164.
[18] P. Alexandridis, J.F. Holzwarth, T.A. Hatton, Macromolecules 27 (1994) 2414–2425.
[19] J.G. Fatou, L. Mandelkern, J. Phys. Chem. 69 (1965) 417–428.
[20] K. Madhavan Nampoothiri, N.R. Nair, R.P. John, Bioresour. Technol. 101 (2010) 8493–8501.
[21] K. Kubota, H. Urabe, Y. Tominaga, S. Fujime, Macromolecules 17 (1984) 2096–2104.
[22] P.J. Wyatt, Anal. Chem. 86 (2014) 7171–7183.
[23] R.A. Khalil, A.H.A. Zarari, Appl. Surf. Sci. 318 (2014) 85–89.
[24] L. Guo, R.H. Colby, M.Y. Lin, G.P. Dado, J. Rheol. 45 (2001) 1223–1243.
[25] T. Sakai, H. Kurosawa, T. Okada, S. Mishima, Colloids Surf., A 389 (2011) 82–89.
[26] R. Wang, T. Hughes, S. Beck, S. Vakil, S. Li, P. Pantano, R.K. Draper, Nanotoxicology 7 (2013) 1272–1281.
[27] L. Illum, S.S. Davis, Life Sci. 40 (1987) 1553–1560.
[28] A. Sukhanova, S. Bozrova, P. Sokolov, M. Berestovoy, A. Karaulov, I. Nabiev, Nanoscale Res. Lett. 13 (2018) 1–21.
[29] S.K. Filippov, A. Bogomolova, L. Kaberov, N. Velychkivska, L. Starovoytova, Z. Cernochova, S.E. Rogers, W.M. Lau, V.V. Khutoryanskiy, M.T. Cook, Langmuir 32 (2016) 5314–5323.
[30] P. Parekh, S. Ohno, S. Yusa, E.V. Lage, M. Casas, I. Sández-Macho, V.K. Aswal, P. Bahadur, J. Phys. Chem. B 120 (2016) 7569–7578.
[31] T. Gan, Y. Guan, Y. Zhang, J. Mater. Chem. 20 (2010) 5937–5944.
[32] Y. Lu, E. Zhang, J. Yang, Z. Cao, Nano Res. 11 (2018) 4985–4998.